Self-Organization of Dipolar 4,4′-Disubstituted 2,2′-Bipyridine Metal Complexes into Luminescent Lamellar Liquid Crystals

Daniela Pucci,*[a] Giovanna Barberio,[a] Alessandra Crispini,[a] Oriano Francescangeli,[b] Mauro Ghedini,[a] and Massimo La Deda[a]

Keywords: N ligands / Platinum / Zinc / Nickel / Metallomesogens

Mononuclear *cis*-dichloro complexes, [L^nMCl_2], with different metal centres (Pt^{II}, Ni^{II}, and Zn^{II}) and a series of palladium and platinum derivatives, [L^2MX_2], in which chloride groups are replaced with iodide, bromide, and azide ligands, have been synthesized from 4,4′-disubstituted-2,2′-bipyridines. Upon complexation of these non-mesogenic ligands, the peculiar structural arrangement, characterized by intermolecular associations of the new derivatives, induces mesomorphism in most [L^2MX_2] complexes, confirming the importance of coordination chemistry in metal-mediated formation of liquid crystals. Single crystal X-ray structures have been determined for dihexadecyl 2,2′-bipyridyl-4,4′-dicarboxylatopalladium and -zinc dichloride derivatives. Both the metal centres and the ancillary ligands have been varied to use dipole coupling as a tool to control molecular architecture: thermal, as well as spectroscopic properties, depend strongly upon molecular dipolar interactions. Tunable red and blue emitters based on Pd^{II} and Pt^{II}, both in solution and in the solid state, have been obtained.

Introduction

"Unconventional" metallomesogens form a new class of liquid crystals that exhibit novel structural and physical properties and numerous strategies have recently been developed for their design. Coordination chemistry has received increasing attention as a metal ion can induce mesomorphism in non-mesomorphic ligands.[1,2]

This phenomenon can be achieved through changes of molecular conformation, shape and structure induced both by complexation[3−6] and association phenomena of different natures, giving rise to supramolecular assemblies.[7−9] We are particularly interested in the so-called complementary shape approach, which is usually adopted to promote columnar mesophases, and we have looked at obtaining novel superstructures in calamitic mesophases by utilising attractive dimeric associations of small molecules with a large central dipole moment. 2,2′-Bipyridines are very attractive ligands because of their extensive coordination chemistry and their versatility: their spectroscopic and chemical properties can be tuned by the choice of metal centre and substituents.[10−14]

We recently reported the synthesis of a new family of non-mesomorphic dialkyl-2,2′-bipyridine-4,4′-dicarboxylates, L^n; the induction of a dipole moment, upon coordination with a $PdCl_2$ moiety, resulted in self-assembling dimers of metallomesogenic [L^nPdCl_2] species **I**−**III**, confirming the role of coordination chemistry in the metal-mediated formation of liquid crystals.[15]

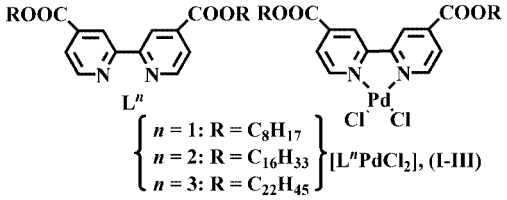

Here we report the crystal structure characterization of the [L^2PdCl_2] (**II**) derivative. The head-to-tail arrangement of the single molecules of this class of complexes is confirmed and the packing and Pd···Pd intermolecular separation within the dimer and between dimers is discussed.

Liquid crystal displays (LCDs), which currently dominate flat panel technology, have severe limitations in brightness and energy efficiency due to the use of absorbing polarizers and color filters which convert a major amount (more than 80%) of the incident light into thermal energy.[16] Photoluminescent materials that act as "active" color filters and, therefore, might enhance the visual performance of LCDs.[17] Although luminescent platinum(II) complexes have attracted much attention recently as possible sen-

[a] LASCAMM, Unità INSTM della Calabria, Dipartimento di Chimica, Università della Calabria, 87030 Arcavacata (CS), Italy
[b] Dipartimento di Fisica e Ingegneria dei Materiali e del Territorio and Istituto Nazionale per la Fisica della Materia, Università di Ancona, Via Brecce Bianche, 60131 Ancona, Italy

sors,[18] photochemical and electroluminescent devices,[19] there are few examples of emitters based on Pd^{II}.[20] Therefore, absorption and fluorescence measurements, in solution and in the condensed state, have been performed on the L^n ligands and the corresponding **I**−**III** palladium complexes. Moreover, to study systematically the effect of structural changes on the dipole moments, intermolecular stacking interactions and supramolecular arrangements, two new classes of the dialkyl 2,2′-bipyridine-4,4′-dicarboxylates metal derivatives have been prepared (**1**−**15**). This paper reports the synthesis and thermal and spectroscopic characterization of a family of *cis*-dichloro complexes $[L^nMCl_2]$ where M is Pt^{II}, Ni^{II}, and Zn^{II}. The crystal structure determination of $[L^2ZnCl_2]$ is also reported. In addition, a series of dihexadecyl 2,2′-bipyridyl-4,4′-dicarboxylate palladium and platinum derivatives $[L^2MX_2]$, in which the chlorine groups are replaced with iodide, bromide, and azide ligands, have also been prepared. Several novel complexes with potential applications as blue and red metallomesogens emitters have been obtained and the correlations between the self-assembling properties of these complexes and their photophysical properties are discussed.

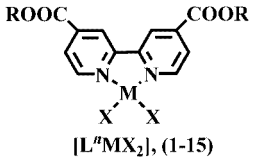

$[L^nMX_2]$, (1-15)

Results and Discussion

Single-Crystal X-ray Diffraction for $[L^2PdCl_2]$ (II·2CHCl$_3$) and $[L^2ZnCl_2]$ (8) Complexes

The structure of **II**·2CHCl$_3$ is shown in Figure 1 and the bond lengths and angles are listed in Table 1.

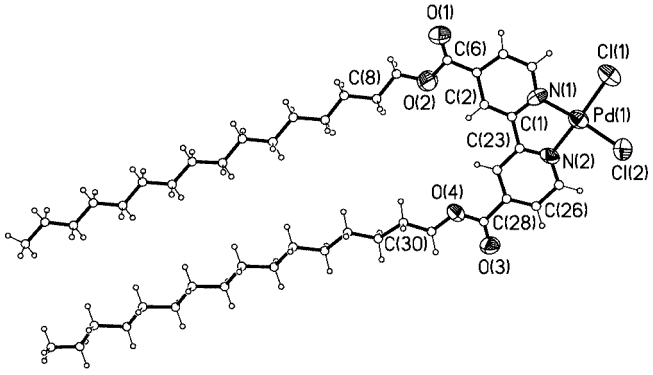

Figure 1. Molecular structure and atomic labeling scheme (50% probability thermal ellipsoids) of complex **II**·2CHCl$_3$

There are two cocrystallized chloroform molecules per complex molecule in the asymmetric unit. The Pd atom has a distorted square-planar geometry with a bite angle N(1)−Pd−N(2) of 81.6(4)°. The bond lengths and angles within the five-membered chelate ring agree well with those reported for other dichlorine palladium(II) species and various substituted 2,2′-bipyridine complexes.[21]

Table 1. Selected bond lengths [Å] and angles [°] for complex **II**·2CHCl$_3$

Pd(1)−N(1)	2.016(10)	Pd(1)−N(2)	2.041(10)
Pd(1)−Cl(1)	2.291(4)	Pd(1)−Cl(2)	2.281(4)
N(1)−Pd(1)−N(2)	81.6(4)	Cl(1)−Pd(1)−Cl(2)	90.7(2)
N(1)−Pd(1)−Cl(1)	95.3(4)	N(1)−Pd(1)−Cl(2)	86.4(2)
N(2)−Pd(1)−Cl(1)	176.8(4)	N(2)−Pd(1)−Cl(2)	92.4(4)

The five-membered chelate ring is essentially planar with a maximum deviation from planarity of 0.03(1) Å [C(1)]. The carboxylic oxygen atoms O(1) and O(3) of the dihexadecyl 2,2′-bipyridine-4,4′-dicarboxylate ligands point in opposite directions, with torsion angles C(2)−C(3)−C(6)−O(1) and C(24)−C(25)−C(28)−O(3) of 165 and 168°, respectively. Hence, the two carboxylic hydrocarbon chains are straight and parallel, and they both have a regular *anti* conformation, with mean torsion angles of 177(2) and 178(2)°, respectively.

The shortest Pd···Pd intermolecular separation of 3.487(2) Å was found between centrosymmetrically related molecules arranged in a head-to-tail fashion, which was approximately superimposed along the *a* axis (Figure 2, a).

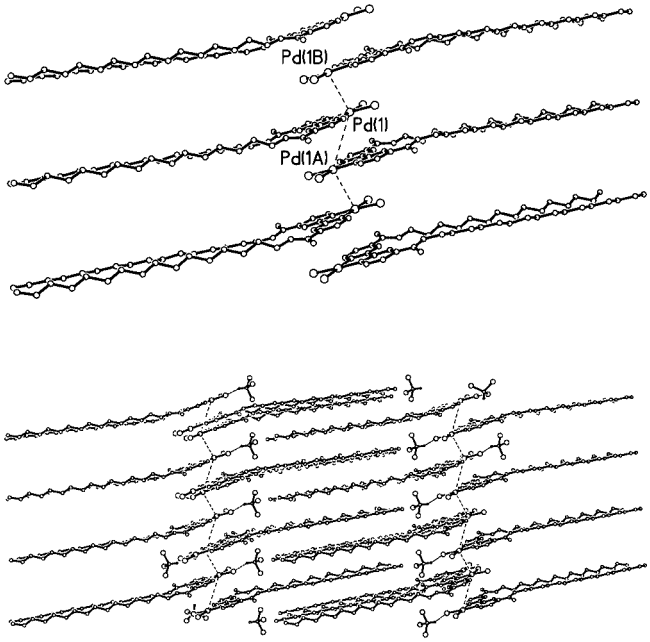

Figure 2. Ball and stick representation of the crystal packing of complex **II**·2CHCl$_3$ (b), viewed along the *b*-axis. Separate view (a) shows the alternating short and long Pd···Pd intermolecular contacts

This distance is similar to a polymorph of the (2,2′-bipyridine)dichloropalladium(II) complex (3.46 Å)[22] and is shorter than other similar complexes containing substituted 2,2′-bipyridine (found in the Cambridge Structural Database, CSD). Within the dimer the Pd···Pd vector deviates slightly from orthogonality to the coordination plane (9° angle with the plane normal), suggesting a very weak at-

tractive character for the Pd···Pd interaction. The coordinated portions of the bipyridine ligands are oriented in opposing directions and thus no significant aromatic π−π stacking within the dimer was observed. In fact, the pyridine rings have interplanar and centroid-centroid distances of 3.44 and 5.91 Å, respectively, and interplanar and displacement angles of 0.4 and 126°, respectively, and a horizontal slip of 4.81 Å.

A second rather longer Pd···Pd separation of 4.778 Å was found between the dimers. The Pd···Pd contacts alternate along a zig-zag chain with an off-set of 1.78 Å [Pd(a)−Pd−Pd(b) 127.5(2)°]. The 3D-space complex **II**·2$CHCl_3$ gives rise to a layered structure (Figure 2, b), where the planar cores (representing the polar, or at least polarizable, part of the molecule), superimposed along one direction, alternate with non-polar chains, confined to a non-polar region. The degree of interdigitation within the paraffinic sublayer is not as high as expected from the segregation effects of the alkyl chains, due to the chloroform molecules that fill the holes between the two sublayers. The resultant calculated interlayer spacing is 31.9 Å.

The overall structure of the analogous complex containing Zn^{II}, **8**, is completely different from the palladium one (Figure 3). As with [Zn(bipy)Cl_2][23] and [Zn(phen)Cl_2],[24] complex **8** is tetrahedral. Bond lengths and angles are listed in Table 2. The neutral complex has a C_2 symmetry axis passing through the zinc ion and the midpoint of the bipyridine ligand.

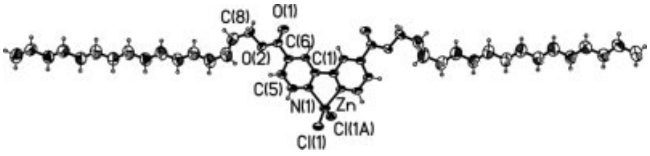

Figure 3. Molecular structure and atomic labeling scheme (50% probability thermal ellipsoids) of complex **8**

Table 2. Selected bond lengths [Å] and angles [°] for complex **8**

Zn−N(1)	2.064(3)	Zn−Cl(1)	2.211(1)
N(1)−Zn−N(1a)	79.5(2)	Cl(1)−Zn−Cl(1a)	123.1(1)
N(1)−Zn−Cl(1)	111.7(1)	N(1a)−Zn−Cl(1)	111.2(1)

The bond lengths and angles are similar to those for [Zn(bipy)Cl_2][23] and other Zn^{II} substituted 2,2′-bipyridine derivatives,[25] and [Zn(phen)Cl_2].[24] Because the zinc is tetrahedral, the $ZnCl_2$ moiety is not coplanar with the mean plane passing through the five-membered chelate ring. The dihedral angles Cl(1)−Zn−N(1)−C(1) and Cl(1a)−Zn−N(1)−C(1) are 107.9(3) and −110.3(3)°, respectively. The two carboxylic oxygen atoms O(1) and O(1a) point towards the internal part of the bipyridine ligand [torsion angle C(2)−C(3)−C(6)−O(1) 6.5(7)°].

Moreover, since O(2)−C(6)−C(7)−C(8) and C(8)−C(9)−C(10)−C(11) torsion angles are in a *gauche* conformation [54.6(7) and −85.2(8)°, respectively), the two carboxylic hydrocarbon chains run in opposite directions.

The dihedral geometry of the zinc ion prevented the formation of dimers in the crystal packing, as observed in the analogous complex **II**, and favour strong intermolecular contacts involving the bipyridine hydrogen atoms that are *ortho* and *meta* with respect to the $ZnCl_2$ moiety.

In fact, while H(4) participates in H···Cl contacts that are shorter than the sum of the van der Waals radii of hydrogen and chlorine atoms [Cl(1)···H(4b) = 2.863(1) Å, C(4b)−H(4b)···Cl(1) = 143.5(3)°, C(4b)···Cl(1) = 3.668(5) Å, b = *x*, 1 − *y*, *z* − 1/2), H(5) showed an hydrogen bond interaction with the carboxylic oxygen atom O(1) [O(1)···H(5c) = 2.424(3) Å, C(5c)−H(5c)···Cl(1) = 158.6(3)°, C(5c)···O(1) = 3.307(5) Å, c = *x*, 1 + *y*, *z*) (Figure 4, a).

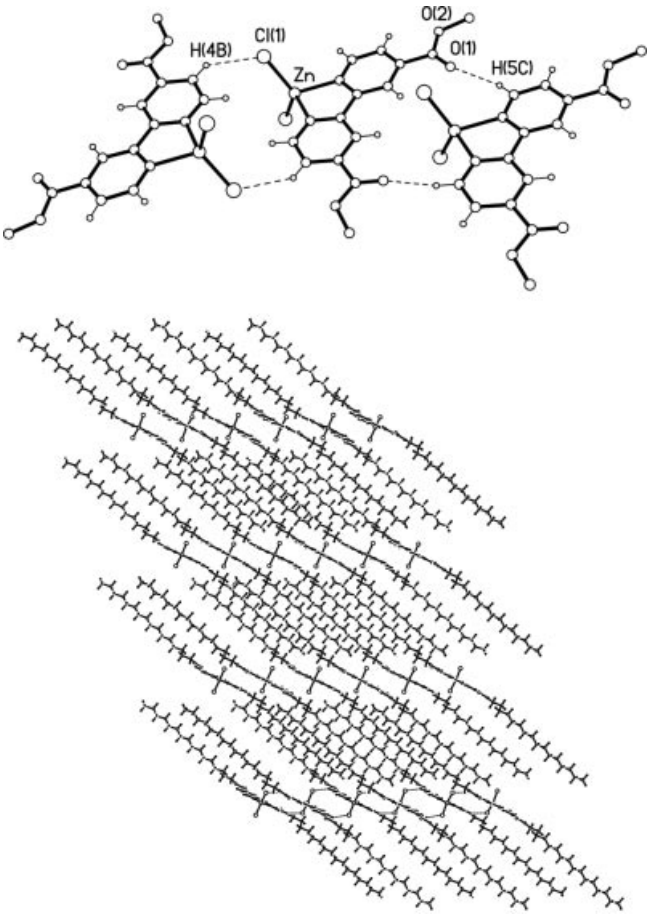

Figure 4. Ball and stick representation of the crystal packing of complex **8** (b), viewed along the *b* axis. Separate view (a) shows the C−H···X (X = Cl, O) intermolecular contacts within the *ac* plane

The crystal packing of **8** is characterized by a layered structure with a calculated interlayer spacing of 19.8 Å (Figure 4, b). Each carboxylic chain of a molecule of **8** is part of each paraffinic sub-layer, in which the segregation effects of the alkyl chains cause a high degree of interdigitation. The long molecular axis is tilted with respect to the layer normal by 56°.

Synthesis

The [L^nMCl_2] complexes **1**−**9** were prepared by the reaction of an equimolar amount of the appropriate L^n ligands with [$Pt(PhCN)_2Cl_2$] (in toluene, under reflux), $NiCl_2$ (in ethanol, under reflux) or $ZnCl_2$ (in dichloromethane, at room temperature) (Scheme 1).

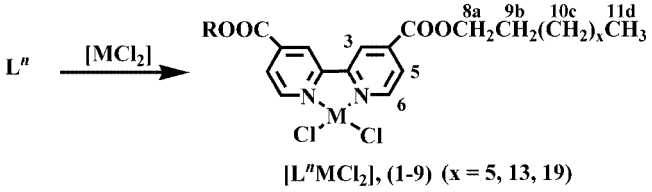

Scheme 1. Synthetic route to [L^nMCl_2] complexes **1**−**9** and related proton numbering scheme. *Reagents and conditions*: *i)* [MCl_2] = [$Pt(PhCN)_2Cl_2$], toluene, ΔT; *ii)* [MCl_2] = $NiCl_2$, ethanol, ΔT; *iii)* [MCl_2] = $ZnCl_2$, dichloromethane, room temp.

The dihexadecyl 2,2′-bipyridyl-4,4′-dicarboxylate palladium and platinum *cis*-dichloro complexes were transformed into the corresponding [L^2MX_2] derivatives by metathetical reactions with potassium iodide (**10**, **11**), potassium bromide (**12**, **13**), and sodium azide (**14**, **15**) (Scheme 2).

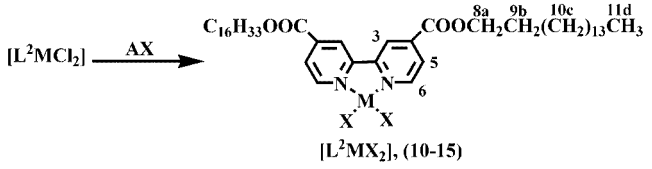

Scheme 2. Synthetic route to [L^2MX_2] complexes **10**−**15** and related proton numbering scheme. *Reagents and conditions*: *i)* AX = KI, acetone, room temp.; *ii)* AX = KBr, DMF, room temp.; *iii)* AX = NaN_3, acetone, room temp.

The structure and purity of all the compounds were confirmed using elemental analyses, IR and ^1H NMR spectroscopy, as reported in the Exp. Sect. For all of the investigated complexes, IR spectra showed ν(COO) absorptions for the carbonyls groups at higher wavenumbers (ca. 20 cm^{-1}) than for the free ligands. Moreover, the azide compounds **14** and **15** showed a strong band at 2043 and 2063 cm^{-1} respectively, due to the asymmetric N_3 stretching vibration, suggesting coordination of the ligand to the metal centre.[26] In the ^1H NMR spectra of the platinum and zinc [L^nMCl_2] complexes the resonance attributable to the $H^{6,6'}$ protons is low-field shifted by about 1 ppm with respect to the organic precursors. These observations confirm the coordination of bipyridines to the metal fragment. In the ^1H NMR spectra of the Ni^{II} complexes the signals are very broad, confirming the assumed distorted square-planar structure induced by the 4,4′ substituents of the bipyridine ligand. The few examples of crystal structures of dihalo disubstituted Ni^{II} complexes show a strong substituent effect on the geometry around the metal ion, with the promotion of distorted square-planar coordinations.[27−29]

Upon exposure to air, **4** and **5** are not stable as solids but gradually adsorbed water, as evidenced by the change from pale green to deep green, IR spectroscopy and elemental analysis.

The ^1H NMR resonance frequencies of the $H^{6,6'}$ protons of the palladium and platinum [L^2MX_2] complexes are very sensitive to the nature of the metal-bonded ancillary groups. This electronic effect of the ligand is seen for **10**−**13** where the $H^{6,6'}$ signal progressively moved downfield (Δδ of ca. 0.3 and 0.6 ppm for the bromo and iodo derivatives, respectively) as the electron-withdrawing power of the X-bridging ligand decreases. For complexes **14** and **15** the $H^{6,6'}$ proton resonances shifted upfield by ca. 0.7 ppm with respect to the homologous signals of the corresponding chloro precursors, as observed in related azido complexes of diimines.[14]

Liquid Crystalline Properties

[L^nMCl_2] Complexes

Although free 2,2′-bipyridine-4,4′-dicarboxylates (L^n) are not liquid crystals, most of their metal complexes [L^nMCl_2] show mesomorphism (investigated by polarized optical microscope and XRD); the phase diagram is shown in Figure 5. Thermal data, obtained using differential scanning calorimetry (DSC), are summarized in Table 3.

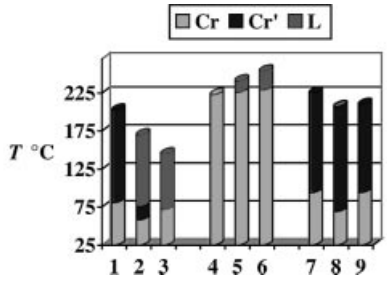

Figure 5. Bar graph showing the mesomorphic behaviour of [L^nMCl_2] (**1**−**9**) complexes

The *cis*-dichloro complexes with the shortest tail (R = C_8H_{16}) melted directly into an isotropic liquid at temperatures higher than for the corresponding free ligand, irrespective of the metal atoms.

The higher homologues of platinum, **2** and **3**, showed a mesophase with a mosaic-like texture (Figure 6), as observed in analogous palladium derivatives.[15]

As expected, the melting and clearing points decreased with aliphatic chain length, ranging from 16 to 22 carbon atoms, and, thus, complex **3** showed a more stable mesomorphism.

The X-ray diffraction (XRD) patterns of platinum complexes **2** and **3** in the mesophase were very similar to those of the analogous palladium complexes **II** and **III**.[15] The XRD pattern of **2** exhibits sharp inner reflections and diffuse outer halos that are consistent with a layered structure (Figure 7).

Table 3. Optical and thermal properties of the [L^{n}MCl$_2$] (**1**−**9**) complexes

Complex	Transition[a]	T[°C]	ΔH[kJ·mol^{-1}]	d[Å]
	Cr − Cr′	80.9	3.8	22.3 (Cr)
1	Cr′ − I	202.35	11.4	23.3 (Cr′)
	I − Cr	201.7	11.0	
	Cr − Cr′	57.8	8.9	31.3 (Cr)
	Cr′ − L	76.0	5.4	34.3 (Cr′)
2	L − I	170.1	13.0	36.5 (L)
	I − L	172.0	12.9	
	L − Cr	59.4	5.3	
	Cr − Cr′	33.8	26.4	
	Cr − L	71.6	41.3	37.3 (Cr)
3	L − I	144.7	5.3	44.0 (L)
	I − L	138.5	5.8	
	L − Cr	64.9	39.8	
4	Cr − I	223.3 dec	11.3	
5	Cr − L	225.6	14.0	
	L − I	233.5	1.9	
6	Cr − L	229.3	15.4	
	L − I	251.4 dec	15.1	
	Cr − Cr′	94.0	4.4	
7	Cr′ − I	224.6	44.9	
	I − Cr	204.2	27.9	
	Cr − Cr′	68.9	37.4	
8	Cr′ − I	207.2	27.9	
	I − Cr′	195.8	36.2	
	Cr′ − Cr	64.4	37.1	
	Cr − Cr′	93.7	91.0	
9	Cr′ − I	210.0	12.7	
	I − Cr′	198.4	26.8	
	Cr′ − Cr	68.3	45.4	

[a] Cr: crystal; L: lamellar; I: isotropic liquid.

Figure 6. Polarized optical micrograph of the mosaic texture for complex **2** at 150 °C.

In fact, the inner reflections consist of a set of *00n* peaks centred at $q = 2\pi n/d$ ($q = 2\pi\sin\theta/\lambda$ is the modulus of the scattering vector, 2θ is the scattering angle), where n is an integer ($n = 1-4$) and $d = 36.7$ Å is the layer spacing. The wide diffuse outer halo centred about $q = 1.3$ Å^{-1} is associated with the short-range liquid-like positional ordering of the hydrocarbon chains. Moreover, two additional peaks appeared, corresponding to $d_1 = 10.5$ Å and $d_2 = 3.4$ Å, which arise from Pt−Pt in-plane correlations along mutually-orthogonal directions which are parallel and orthogonal, respectively, to the long side of the molecular core (i.e. the axis of the benzene rings). This type of XRD pattern is consistent with an ordered smectic phase with one-dimensional ordering of the molecules within the layers as well as a lamello-columnar mesophase without positional correlation between the layers. Because the spacing of the layers in this compound is larger than the calculated molecular length in the fully extended configuration ($L \approx 28$ Å), but smaller than $2L$ ($d/L \approx 1.3$), if we assume that the arrangement is of a smectic type, the molecules are not arranged in single molecular layers but organized in semi-bilayers that are partially interdigitated, giving rise to a bilayered SmA$_d$ phase.[30] Here the semi-bilayer ordering is caused by dipole−dipole interactions and antiparallel correlations of nearest neighbour molecules, characterised by short intermetallic M···M distances (Figure 8).

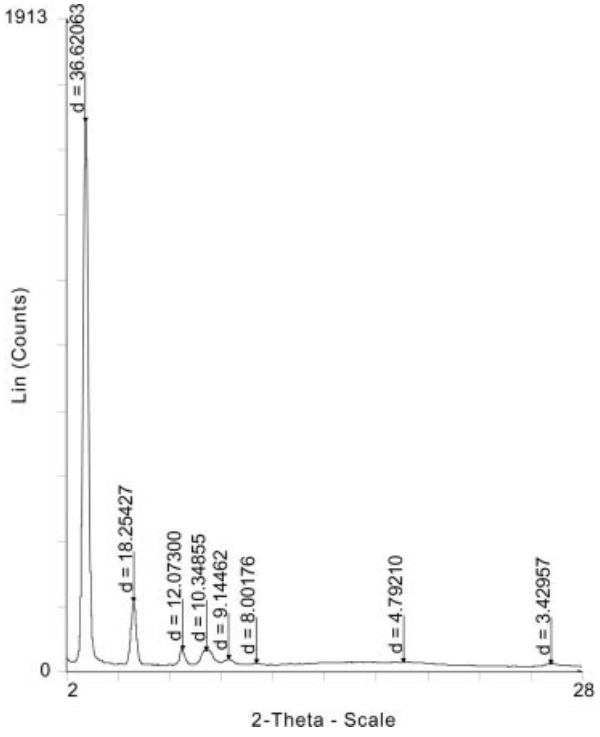

Figure 7. XRD pattern of the smectic phase of complex **2** recorded at $T = 140$ °C

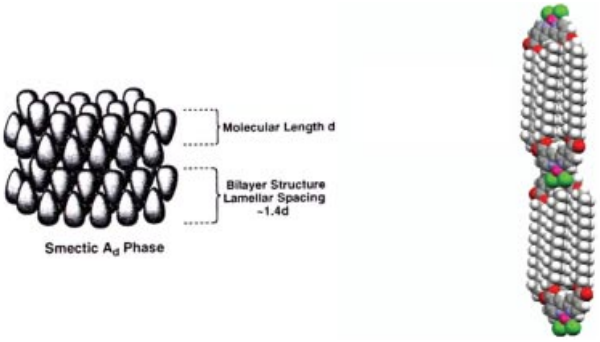

Figure 8. Idealized molecular arrangement for complex **2** in the SmAd phase

However, a very similar XRD pattern has been reported for *ortho*-palladated 5,5′-dialkyl-2,2′-bipyridines, where it was concluded that the mesophase, although showing a schlieren texture, was a lamello-columnar phase, with aromatic cores stacked in columns and in close contact with one another to form defined layers.[31]

Therefore, even for our complexes, the lamellar structure in the mesophase could be described as columnar. In this case the flat molecular cores of each molecule would be stacked along the *a* direction to form columns that would be in close contact with one another to form layers. The repetition of these layers (separated by the disordered aliphatic chains) along the *c* direction would give rise to a periodic structure (Figure 9).

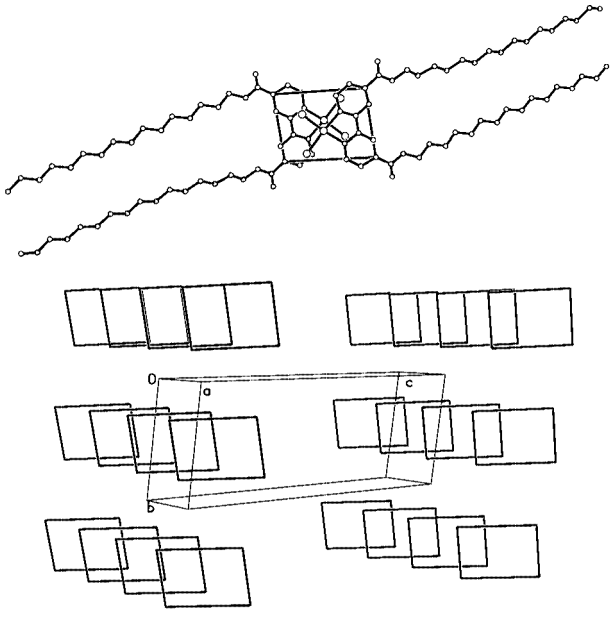

Figure 9. Schematic view of the molecular packing of complex **2** showing the stacking of the aromatic cores

In summary, since the XRD patterns of complexes **2** and **3** agree with both assignments (SmAd or lamello-columnar) and because the literature lacks a typical texture for the SmAd mesophase, while different textures are associated with a lamello-columnar phase,[31−33] we shall refer to this phase as L.

Ni^{II} compounds **5** and **6** showed a layered mesophase whose high transition temperatures prevented a complete identification by optical microscopy and X-ray powdered diffraction. Thermal analysis of Ni^{II} complexes on fresh samples and on samples stored in air for some days confirmed the addition of molecules of water. None of the zinc complexes were mesomorphic: after a crystal-to-crystal transition they melted into the isotropic liquid at temperatures much higher than the corresponding organic precursor. For **8** and **9** the total loss of liquid crystalline properties was ascribed to the tetrahedral coordination, which promoted strong intermolecular interactions in the crystal packing other than the metal−metal ones observed in the square-planar derivatives.

Both melting and clearing points, as expected, depended mostly on the aliphatic chains but were also very sensitive to the metal atom and the core interactions. Comparison of the thermal properties of complexes **1**−**6** with those reported for palladium(II)[15] shows that the melting temperatures, in each series, decreased in the order Pt < Pd < Ni whereas for the clearing points the trend was Pd < Pt < Ni, illustrating that the platinum derivatives have the largest mesomorphic range.

$[L^2MX_2]$ Complexes

All the dihexadecyl 2,2′-bipyridyl-4,4′-dicarboxylate palladium and platinum derivatives $[L^2MX_2]$ displayed enantiotropic liquid crystalline behaviour and were investigated by polarized optical microscope and XRD. The phase diagram is shown in Figure 10. The thermal data of $[L^2MX_2]$ complexes, as measured using DSC, are summarized in Table 4.

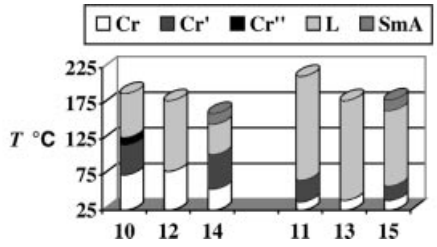

Figure 10. Bar graph showing the mesomorphic behaviour of $[L^2MX_2]$ (**10**−**15**) complexes

The phase sequence is notably dependent on the ancillary ligands overcoming the effect of the different metal atoms, which directly influence the thermal ranges. In particular, the iodo complexes **10** and **11**, after a crystal-to-crystal transition, gave rise to an L phase with the same mosaic texture as the chloro precursors. The thermotropic behaviour of the bromo derivatives **12** and **13** was also characterized as an L phase whose texture is retained, on cooling, in the solid state. The substitution of chloro for bromo atoms did not lead to crystal-to-crystal transitions. The mesomorphic properties were slightly changed when azide groups replaced the chloride ligands. When heated, complexes **14** and **15** gave, in addition to the crystal-to-crystal and the crystal-to-L transitions, an L-SmA transition phase, as confirmed by XRD analysis. For the chloro, iodo, and bromo complexes the layer thickness in the L phase increases with temperature due to an increase in molecular mobility and a progressive decrease in the degree of orientational order. This behaviour was magnified in the azide complexes. Indeed, in the high-temperature SmA phase the peaks corresponding to $d_1 \approx 10.5$ Å disappeared. These results suggest that, in this mesophase, thermal disorder within the layer weakened the intermolecular dipole interactions. In complexes **14** and **15**, on cooling the isotropic liquid, the SmA phase was observed, *via batonnets*, turning into a focal-conic texture and then homeotropic. On further cooling the L phase is restored, with a schlieren texture, which remained until solidification.

Table 4. Optical and thermal properties of the [L^2MX_2] (**10**−**15**) complexes

Complex	Transition[a]	T [°C]	ΔH [kJ·mol^{-1}]	d [Å]
	Cr − Cr′	75.1	55.6	30.1 (Cr)
	Cr′ − Cr′′	116.7	0.5	34.2 (Cr′′)
	Cr′′ − L	123.6	2.3	36.5 (L)
10	L − I	186.1	19.0	
	I − L	184.2	18.6	
	L − Cr′	116.6	2.8	
	Cr′ − Cr	62.4	50.5	
	Cr − Cr′	36.8	8.4	30.0 (Cr)
	Cr′ − L	67.3	38.8	35.9 (L)
11	L − I	212.2	19.6	
	I − L	211.8	20.3	
	L − Cr	51.5	35.7	
	Cr − Cr′	38.8	5.5	
	Cr − L	79.6	53.0	36.5 (L)
12	L − I	178.5	13.6	
	I − L	178.0	12.5	
	L − Cr	41.9	24.8	
	Cr − L	39.2	15.0	32.5 (Cr)
13	L − I	179.0	1.8	36.0 (L)
	I − L	178.0	3.0	
	L − Cr	37.3	9.4	
	Cr − Cr′	55.2	24.5	36.7 (Cr)
	Cr′ − L	103.2	17.1	37.1 (Cr′)
	L − SmA	145.6	2.4	37.3 (L)
14	SmA − I	159.3	9.3	34.1 (SmA)
	I − SmA	154.2	7.6	
	SmA − L	144.2[b]	//	
	L − Cr	26.9	39.0	35.7 (L)
				37.7 (Cr)
	Cr − Cr′	39.1	20.1	34.0 (Cr)
	Cr′ − L	58.5	1.2	37.7 (L)
	L − SmA	164.7	1.5	
15	SmA − I	169.5	2.7	
	I − SmA	160.9	2.1	
	SmA − L	150.0[b]	//	
	L − Cr	35.2	2.7	

[a] Cr: crystal; L: lamellar; Sm: smectic; I: isotropic liquid. [b] Data by optical observation.

For all palladium and platinum complexes **10**−**15** the mesomorphic behaviour depends on the size of X and on the dipole moment associated with the M−X bond, irrespective of the metal atom. Indeed, the mesophase appeared at increasing temperatures in the order Br < I < Cl while the sequence for the clearing points was Cl < Br < I. However, with respect to the halo-compounds, the azide group promoted a lowering of both transition temperatures.

Finally, regardless of the X group, compared to the corresponding palladium compounds, the platinum complexes formed more stable mesophases, exhibiting, on average, much lower melting points and higher clearing temperatures.

Photophysical Studies − Absorption and Emission Spectroscopy

Uncomplexed Bipyridine Ligands

The absorption spectra of L^n ligands, in solution, were unaffected by their chain length, all showing a strong band at 300 nm with a shoulder at about 315 nm, attributed to a spin-allowed π→π* transitions involving the aromatic rings. At longer wavelengths a weakly absorbing tail at about 340 nm was assigned to an n→π* transition, probably involving pyridine nitrogens and ester fragments (Table 5). With respect to the unsubstituted bipyridine, the electron-withdrawing carboxylate groups induced a red-shift of the absorption bands, as determined by the LUMO stabilization.[34] The electronic spectra recorded from microcrystalline samples of L^n were identical to those in solution, indicating the absence of any relevant interactions in the solid state that can modify the energy states.

Table 5. Absorption data; MLCT bands are typed in bold

Compound	Solution (CH_2Cl_2) Abs., λ_{max}/nm (ε/M^{-1}·cm^{-1})	Solid (KBr pellet) Abs., λ_{max}/nm
L^2	300 (6700), 315 (sh), 340 (sh)	300
II	320 (sh), 330 (18700), **355 (2900)**	335
2	300 (15100), 320 (sh), 340 (6350), 360 (sh), 400 (sh), **422 (4400)**, 450 (sh)	300, **433**
5	314 (13500), 324 (14000)	322
8	314 (16700), 324 (19500)	322
10	320 (18000), 334 (17400), 350 (sh), **394 (4000)**, 496 (2600)	320, 500
11	316 (21400), 330 (sh), 360 (sh), **460 (5800)**, 525 (sh)	300, **480**
12	320 (sh), 332 (17300), **360 (3100)**	340
13	305 (14700), 340 (sh), 360 (sh), **432 (3300)**, 470 (sh)	310, **440**
14	304 (21400), 315 (sh), 332 (13700), **377 (4100)**	300, **390**
15	312 (20050), 330 (sh), 350 (sh), 440 (sh), **455 (4550)**, 500 (sh)	300, **460**

The ligand L^2 exhibited UV luminescence (Table 6) when excited on the π→π* absorption band (quantum yield of L^2 7.5%). Because of the energy and quantum yield, the emission was assigned to the singlet π→π* excited state.

Table 6. Photophysical data (Em. = Emission)

Compound	Solution (CH_2Cl_2) Em., λ_{max}/nm	Φ (%)	Solid (KBr pellet) Em., λ_{max}/nm
L^2	350	7.5	300
II	n.o.	−	456
2	482	$< 10^{-2}$	640
15	640	0.65	n.o.

[L^2MCl_2] Complexes

Preliminary investigation of the [L^nMCl_2] complexes revealed that the photophysical characteristics remained constant despite variation in the chain length of the ligands. Consequently, only the L^2 complexes will be discussed.

The absorption spectrum of **2** in solution (Figure 11 and Table 5) clearly showed two well-defined bands, centred at 300 and 422 nm, and a series of shoulders.

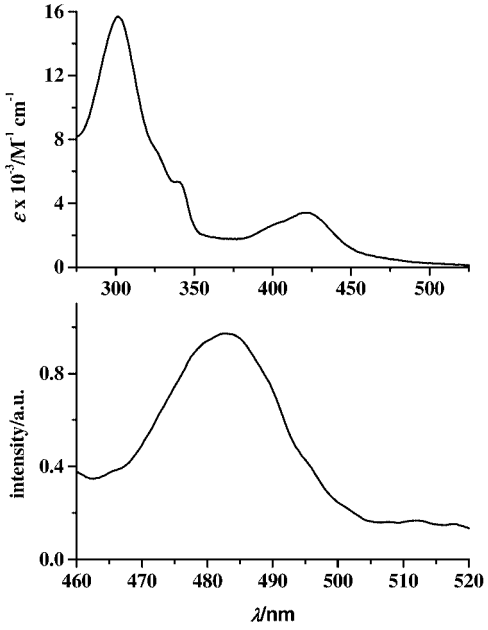

Figure 11. Absorption (top) and emission (down) spectra of complex **2** in dichloromethane solution

In accord with the literature,[35−37] the intense band at 300 nm, with a shoulder at about 320 nm, was attributed to spin-allowed ligand-centred transitions (^{1}LC). The band at 422 nm and its shoulder at about 430 nm could be attributed to ^{1}MLCT and ^{3}MLCT transitions, respectively.[38] A metal-perturbed LC transition could be give the band at 340 nm, while spin-allowed ligand field transitions (LF) produce weak shoulders at about 360 nm.[39]

The electronic spectrum of microcrystalline samples of **2** (Table 5) is not well resolved, due to the reflecting properties of the KBr support, which reduced signal intensity; it is possible to distinguish the principal maxima at 300 and 433 nm, with the first due to an ^{1}LC transition and the second to a ^{1}MLCT. The red-shift of this band was attributed to the environment sensitivity of this type of transition on passing from solution to the solid state.

As expected, the absorption spectrum of **II** (Table 5) did not show a MLCT band in the visible region, since the palladium(II) centre is more difficult to oxidize than the platinum(II) centre. Therefore, the observed UV-band at 355 nm could be assigned to a MLCT transition. The absorption spectrum of complex **II**, recorded from the KBr pellet, showed a 335 nm band corresponding to LC excitation.

The absorption spectra of **5** and **8** are very similar: in the near-UV region both exhibit two maxima at 314 and 324 nm in dichloromethane solution with a single peak at 322 nm in the solid state (Table 5). These features are assigned to the metal-perturbed ligand centred transition, showing two vibronic components in solution.

Complex **2** in dichloromethane solution has an emission band centred at 482 nm (Figure 11 and Table 6), as confirmed by the excitation spectrum.

This band can be attributed to a low-yield ($\Phi < 10^{-2}$ %) radiative deactivation from an ^{1}LF excited state. As expected, the analogous palladium complex **II**, in solution, did not emit, due to low-lying metal-centred excited states (MC), which can be populated easily by thermal activation and provide fast deactivation pathways via molecular distortion.[40]

The solid-state luminescence behaviours of **2** and **II** show interesting differences (Figure 12 and Table 6).

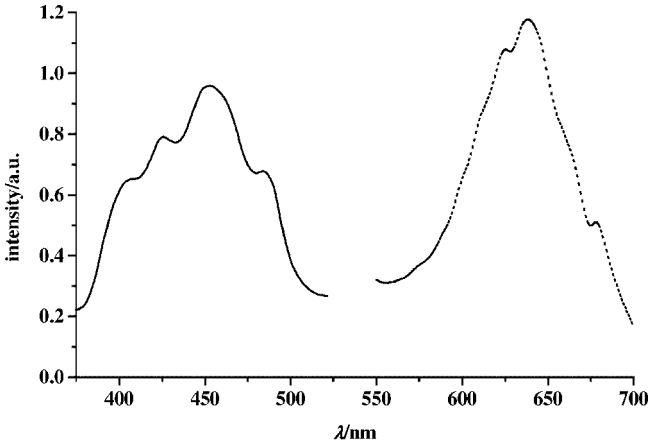

Figure 12. Emission spectra of complex **2** (dotted line) and complex **II** (solid line) in microcrystalline samples

Comparing the emission maximum of **2** in the solid state to that in solution, it is evident that d_z^2(Pt) orbital interactions in the stacked complexes in the microcrystalline sample are strong enough to affect the photophysical properties of the molecules. Therefore a Pt−Pt distance similar to the yellow form of (2,2′-bipyridine)dichloroplatinum(II) can be assumed.[41−43] The structured emission band at about 456 nm in the microcrystalline emission spectrum of **II** seems to indicate that the bipyridyl ligand is involved in the formation of the state responsible for the luminescence.[42] Moreover, the shortest Pd···Pd intermolecular separation of 3.487(2) Å, observed in the X-ray crystal structure determination, does not seem to be strong enough to affect the photophysical properties of the "isolated" molecules. This accounts for a small contribution of the metal in the electronic transition, in which LC character could be mixed with LF transitions. Further studies are necessary to clarify this crucial point.

[L^{n}MX$_2$] Complexes

The origin and position of the bands in the electronic spectra of [L^{2}MX$_2$] can be accounted for in the same way as for the [L^{2}MCl$_2$] spectra, irrespective of X. However, by modifying the donor character of X the MLCT state energy can be adjusted and, consequently, MLCT bands fall in the ranges 355−394 nm and 422−460 nm for the palladium and platinum derivatives, respectively. As discussed above,

the weak fluorescence of **2** in solution is due to the emission from a ^{1}LF state, while the ^{1}MLCT state was deactivated by intersystem crossing (i.s.c.) to the ^{3}MLCT state. For **11** and **13** no luminescence was observed in solution at room temperature. This may be ascribable to the heavy atom effect which, favouring i.s.c. to the ^{3}MLCT state, quenched the fluorescence more efficiently than in **2**. With the complex bearing the azide ligands, **15**, an interesting emission at 640 nm was recorded. This complex did not undergo i.s.c, and a spin-allowed emission from the ^{1}MLCT state was now observed, whereby the photoluminescence quantum yield is higher than that of the ^{1}LF emission (0.65 vs. 0.02 %, respectively).

Although emission was expected in microcrystalline **11**, by analogy with that reported for [(bipy)PtI_2] luminescence,[42] it was not possible to detect it as scattered light fell in the observed spectral range. Likewise, it was difficult to record a clear emission spectrum from the microcrystalline **15** sample, in which emission could be self-quenched by dimeric interactions.

Finally, it was very difficult to assign the low-energy band in the electronic spectrum of **10**, which showed a peak at 496 nm that probably resulted from a mixed triplet−singlet state, favouring spin−orbit coupling.[37] As expected, no emission was detected from solution and microcrystalline samples of palladium complexes **10**, **12**, **14** with X = Br, N_3, I, respectively.

Conclusions

We have further characterized a recently reported[15] series of non-mesogenic dialkyl 2,2′-bipyridine-4,4′-dicarboxylates, L^n, and their *cis*-dichloro palladium liquid crystalline derivatives. Preliminary XRD experiments on the mesophase of the [L^n$PdCl_2$] complexes led us to propose a model in which the promotion of a dipole moment upon complexation induces self-assembling in dimers with antiparallel disposition. The aggregation of each pair of molecules into a layered structure affords a lamellar L phase.[15] This arrangement in the crystalline state has been confirmed by single-crystal X-ray diffraction analysis of the [L^2$PdCl_2$] derivative, **II**. A relatively short Pd···Pd intermolecular separation of 3.487(2) Å is found between centrosymmetrically related molecules arranged in a head-to-tail fashion. Pd···Pd contacts of 4.778 Å between dimers, alternating along a zig-zag chain, give rise to a layered structure. The solid-state luminescence at room temperature of complex **II** is shifted to the violet region with respect to the corresponding ligand.

The synthesis and characterization of two new series of complexes are also described: the *cis*-dichloro compounds [L^nMCl_2], where the palladium is replaced with Pt, Ni, and Zn, and the dihexadecyl 2,2′-bipyridyl-4,4′-dicarboxylate palladium and platinum derivatives, [L^2MX_2], in which the chloride groups are replaced with iodide, bromide, and azide ligands. Careful choice of the molecular building blocks with suitable shapes and geometries enable control of the supramolecular structure, and prediction of the nature of the induced thermal behaviour. Most of the [L^nMX_2] complexes retained the enantiotropic lamellar L phase of the chloro palladium derivatives, while the thermal and spectroscopic behaviour depend on molecular assemblies and thus on electronic and steric factors. In particular, the appearance of mesomorphism is related to the length of the alkyl chains, with long chains (n = 12, 16) producing the global rod-like shape responsible for the liquid crystalline behaviour. Comparing the *cis*-dichloro derivatives containing the same aliphatic tails, their mesomorphic behaviour is directly related to the nature of the metal centre. A single-crystal X-ray structure has been determined for the dihexadecyl 2,2′-bipyridyl-4,4′-dicarboxylate zinc derivative **8**: the tetrahedral geometry prevented dimer formation in the crystal packing and favoured intermolecular contacts that are too strong to induce mesomorphic behaviour. Conversely, the distorted square-planar nickel complexes displayed a lamellar phase at temperatures higher than for the palladium and platinum homologous. For all square-planar complexes the ancillary ligands were varied to use dipole coupling as a tool of molecular architecture. All complexes exhibited the same L phase, but both thermal and spectroscopic properties appeared to depend strongly upon the molecular dipolar interactions.

New photoluminescent metallomesogens have been obtained that display highly desirable optical properties such as a good degree of tunability. The band due to the ^{1}MLCT transition red-shifts, increasing the π-donor capacity of the X ligands, and most of these compounds, including the palladium derivatives, exhibit excellent luminescence properties. Interestingly, the platinum compound bearing chloride ligands is a blue emitter in solution but a red emitter in the solid state. With the azide group, however, the platinum complex is a red emitter in solution but is not an emitter at all in the solid state.

Experimental Section

Materials and Methods: All chemical, reagents and solvents were used as received from commercial sources without further purification. Ligands (L^n) were synthesized as previously reported.[15]

Infrared spectra were recorded on a Perkin-Elmer FT 2000 spectrophotometer and the ^{1}H NMR spectra were recorded on a Bruker WH-300 spectrometer in $CDCl_3$ solution, with TMS as internal standard. Elemental analyses were performed with a Perkin−Elmer 2400 analyzer. The textures of the mesophases were studied with a Zeiss Axioscope polarizing microscope equipped with a Linkam CO 600 heating stage. The transition temperatures and enthalpies were measured on a Perkin−Elmer Pyris 1 Differential Scanning Calorimeter with a heating and cooling rate of 10 °C/min. The apparatus was calibrated with indium. Two or more heating/cooling cycles were performed on each sample.

Spectrofluorimetric grade solvent (Acros Organics) was used for the photophysical investigations in solution at room temperature. Solid-state spectra were obtained from microcrystalline samples on KBr pellets. Absorption spectra were recorded with a Perkin−Elmer Lambda 900 spectrophotometer; uncorrected emis-

sion spectra were obtained with a Perkin-Elmer LS-50B spectrofluorimeter. Fluorescence quantum yields in solution were measured by the method described by Demas and Crosby[44] using [Ru(bipy)$_3$]Cl$_2$ (bipy = 2,2′-bipyridine, $\Phi = 0.028$ in aerated water)[45] as standard. The experimental uncertainty on the band maximum for absorption and luminescence spectra is 2 nm; that on the luminescence intensity is 20% and that on the molar absorption coefficient is 10%. The free ligand and its metal complexes are fairly stable in CH_2Cl_2, as demonstrated by the constancy of their absorption spectra over a week.

The X-ray powder diffraction patterns were obtained using a Bruker AXS General Area Detector Diffraction System (D8 Discover with GADDS). Monochromatized Cu-$K\alpha$ radiation (λ = 1.54 Å) impinged on the about 1 mm thick sample, the temperature of which was controlled to ±0.1° by a hot stage containing electrical resistors.

Crystal Structure Studies: Pale yellow needles of [L^{2}PdCl$_2$] (**II**) with a relatively poor crystal habit were crystallized at room temperature from a chloroform/ethanol mixture. Different crystallization conditions gave no better results. A needle of suitable dimensions was mounted in a fiber glass capillary to avoid solvent evaporation during data collection. Crystal data of [L^{2}ZnCl$_2$] (**8**) were collected on a white, thin plate crystal obtained from a chloroform/ethanol mixture. In both cases diffraction measurements were carried out at room temperature on a Siemens *R3m/V* automated four-circle diffractometer equipped with graphite-monochromated Mo-K_α radiation (λ = 0.71073 Å). The data were corrected for Lorentz, polarization and X-ray absorption effects. For **8** an empirical absorption correction was applied using a method based upon azimuthal (Ψ) scan data.[46] With **II**·2CHCl$_3$ a slow loss of cocrystallized solvent prevented this type of data correction. Therefore the data were corrected for X-ray absorption effects using the *XABS2* program.[47] Details of the crystal data collections are listed in Table 7.

Both structure solutions (Patterson method) and full-matrix least-squares refinements based on F^2 were performed with *SHELXS*/*L* programs of the *SHELXTL-NT* software package (Version 5.10).[48]

For **II**·2CHCl$_3$, only palladium, chlorine (excluding the chlorine atoms of the two co-crystallized chloroform molecules), nitrogen and oxygen atoms were refined anisotropically, for **8**, however, all non-hydrogen atoms were refined anisotropically. In both cases hydrogen atoms were included as idealized atoms riding on the respective carbon atom hybridisation. The bipyridine hydrogen atoms of **8** were included in the refinement in their observed positions.

Synthesis of [L^{n}PtCl$_2$] Complexes 1−3: The [L^{n}PtCl$_2$] derivatives were prepared by the procedure described for the analogous palladium complexes,[15] starting from the suitable ligand and varying the solvent and reaction time for more energetic reaction conditions. The synthesis of [L^{1}PtCl$_2$] (**1**) is detailed below; all other homologues were prepared in a similar fashion and only yields, solvents, ^{1}H NMR, IR, and analytical data are reported.

(Dioctyl 2,2′-Bipyridyl-4,4′-dicarboxylate)platinum(II) Chloride ([L^{1}PtCl$_2$], 1): A solution of [Pt(PhCN)$_2$Cl$_2$] (0.1 g, 0.213 mmol) and dioctyl 2,2′-bipyridine-4,4′-dicarboxylate, L^1, (0.1 g, 0.213 mmol) in toluene (12 mL) was heated at reflux for 24 h. The solvent was then evaporated and the residue recrystallized from dichloromethane/methanol to give a yellow solid complex (0.092 g, 59%). Thermotropic behaviour: Table 3. ^{1}H NMR (300 MHz, CDCl$_3$, 25 °C, ppm): δ = 0.82 (m, 6 H, H$^{11d,11d'}$), 1.23 (m, 20 H, H$^{10c,10c'}$), 1.78 (m, 4 H, H$^{9b,9b'}$), 4.40 (t, ^3J = 6.8 Hz, 4 H, H$^{8a,8a'}$), 8.02 (dd, $^3J_{H,H}$ = 6.2, $^4J_{H,H}$ = 1.7 Hz, 2 H, H$^{5,5'}$), 8.54 (s, 2 H, H$^{3,3'}$), 9.77 (d, $^3J_{H,H}$ = 6.2 Hz, 2 H, H$^{6,6'}$). FTIR (KBr, cm^{-1}):

Table 7. Crystal and structure refinements for complexes **II**·2CHCl$_3$ and **8**

Empirical formula	$C_{44}H_{72}Cl_2N_2O_4Pd.2CHCl_3$ (**II**·2CHCl$_3$)	$C_{44}H_{72}Cl_2N_2O_4Zn$ (**8**)
Molecular mass	1109.1	829.3
Temperature [K]	298	298
Wavelength [Å]	0.71073	0.71073
Crystal system	triclinic	monoclinic
Space group	$P\bar{1}$	$C2/c$
a [Å]	7.436(2)	41.228(8)
b [Å]	11.917(3)	7.937(2)
c [Å]	31.869(13)	14.689(3)
α [°]	92.28(3)	90
β [°]	92.78(3)	107.71(3)
γ [°]	96.72(2)	90
V [Å^3]	2798(1)	4579(2)
Z	2	4
Density [Mg/m^{-3}]	1.316	1.203
Absorption Coefficient [mm^{-1}]	0.752	0.693
F(000)	1156	1784
No. indep. refl.	5966 [R(int) = 0.071]	4058 [R(int) = 0.032]
No. obs. refl.	2012	2107
Data / restraints / parameters	5966 / 0 / 157	4058 / 0 / 240
R_1[a] [$I > 2\sigma(I)$]	0.0779	0.0552
wR_2[b]	0.1133	0.1294
Goodness-of-fit on F^2	0.976	0.870
Largest diff. peak and hole [e·Å^{-3}]	0.457 and −0.575	0.472 and −0.536

[a] $R1 = \Sigma(|F_o| - |F_c|)/\Sigma|F_o|$. [b] $wR2 = \{\Sigma[w(F_o^2 - F_c^2)^2]/\Sigma[w(F_o^2)^2]\}^{1/2}$.

ν(C=O) 1730. $C_{28}H_{40}Cl_2N_2O_4Pt$ (734.62): calcd. C 45.78, H 5.49, N 3.81; found C 45.25, H 5.61, N 3.30.

(Dihexadecyl 2,2′-Bipyridyl-4,4′-dicarboxylate)platinum(II) Chloride ([L²PtCl₂], 2): Yield: 0.076 g, 55%. Recrystallized from dichloromethane/light petroleum; thermotropic behaviour: Table 3. ^{1}H NMR (300 MHz, $CDCl_3$, 25 °C, ppm): δ = 0.88 (t, $^3J_{H,H}$ = 6.7 Hz, 6 H, $H^{11d,11d'}$), 1.26 (m, 52 H, $H^{10c,10c'}$), 1.86 (m, 4 H, $H^{9b,9b'}$), 4.47 (t, $^3J_{H,H}$ = 6.8 Hz, 4 H, $H^{8a,8a'}$), 8.10 (d, $^3J_{H,H}$ = 6.1 Hz, 2 H, $H^{5,5'}$), 8.61 (d, $^4J_{H,H}$ = 1.7 Hz, 2 H, $H^{3,3'}$), 9.88 (d, $^3J_{H,H}$ = 6.1 Hz, 2 H, $H^{6,6'}$). FTIR (KBr, cm^{-1}): ν(C=O) 1730. $C_{44}H_{72}Cl_2N_2O_4Pt$ (959.05): calcd. C 55.10, H 7.57, N 2.92; found C 54.82, H 7.57, N 3.01.

(Didocosyl 2,2′-Bipyridyl-4,4′-dicarboxylate)platinum(II) Chloride ([L³PtCl₂], 3): Yield: 0.076 g, 58%. Recrystallized from dichloromethane/diethyl ether; thermotropic behaviour: Table 3. ^{1}H NMR (300 MHz, $CDCl_3$, 25 °C, ppm): δ = 0.88 (t, $^3J_{H,H}$ = 6.5 Hz, 6 H, $H^{11d,11d'}$), 1.27 (m, 76 H, $H^{10c,10c'}$), 1.86 (m, 4 H, $H^{9b,9b'}$), 4.47 (t, $^3J_{H,H}$ = 6.5 Hz, 4 H, $H^{8a,8a'}$), 8.11 (d, $^3J_{H,H}$ = 6.3 Hz, 2 H, $H^{5,5'}$), 8.61 (s, 2 H, $H^{3,3'}$), 9.94 (d, $^3J_{H,H}$ = 6.3 Hz, 2 H, $H^{6,6'}$). FTIR (KBr, cm^{-1}): ν(C=O) 1733. $C_{56}H_{96}Cl_2N_2O_4Pt$ (1127.37): calcd. C 59.66, H 8.58, N 2.48; found C 59.24, H 9.02, N 2.68.

Synthesis of [L″NiCl₂] Complexes 4−6: The preparation of [L^1NiCl$_2$] (**4**) complex is detailed below; all other homologues were prepared in a similar fashion and only yields, solvents, ^{1}H NMR, IR, and analytical data are reported.

(Dioctyl 2,2′-Bipyridyl-4,4′-dicarboxylate)nickel(II) Chloride ([L¹NiCl₂], 4): A solution of $NiCl_2$ (0.041 g, 0.32 mmol) and dioctyl 2,2′-bipyridine-4,4′-dicarboxylate, L^1, (0.150 g, 0.32 mmol) in ethanol (25 mL) was heated at reflux for 48 h. The solvent was evaporated and the residue recrystallized from dichloromethane/diethyl ether to give a green solid (0.179 g, 94%). Thermotropic behaviour: Table 3. FTIR (KBr, cm^{-1}): ν(C=O) 1729. $C_{28}H_{40}Cl_2N_2NiO_4$ (598.24): calcd. C 56.22, H 6.74, N 4.68; found C 56.83, H 6.44, N 5.02.

(Dihexadecyl 2,2′-Bipyridyl-4,4′-dicarboxylate)nickel(II) Chloride ([L²NiCl₂], 5): 24 h. Yield: 0.159 g, 89%. Thermotropic behaviour: Table 3. FTIR (KBr, cm^{-1}): ν(C=O) 1725. $C_{44}H_{72}Cl_2N_2NiO_4$ (822.67): calcd. C 64.24, H 8.82, N 3.41; found C 64.34, H 8.94, N, 3.77.

(Didocosyl 2,2′-Bipyridyl-4,4′-dicarboxylate)nickel(II) Chloride ([L³NiCl₂], 6): 24 h. Yield: 0.130 g, 75%. Thermotropic behaviour: Table 3. FTIR (KBr, cm^{-1}): ν(C=O) 1725. $C_{56}H_{96}Cl_2N_2NiO_4$ (990.99): calcd. C 67.87, H 9.76, N 2.83; found C 67.77, H 9.09, N 2.90.

Synthesis of [L″ZnCl₂] Complexes 7−9: Compound [L^1ZnCl$_2$] (**7**) was prepared as detailed below; all other homologues were prepared in a similar fashion and only yields, solvents, ^{1}H NMR, IR, and analytical data are reported.

(Dioctyl 2,2′-Bipyridyl-4,4′-dicarboxylate)zinc Chloride ([L¹ZnCl₂], 7): Zinc chloride (0.02 g, 0.171 mmol) was added to a solution of dioctyl 2,2′-bipyridine-4,4′-dicarboxylate, L^1, (0.08 g, 0.171 mmol) in dichloromethane (10 mL). The resultant suspension was stirred at room temperature for 4 days. The solvent was then evaporated and the residue recrystallized from dichloromethane/diethyl ether to give a white solid (0.080 g, 78%). Thermotropic behaviour: Table 3. ^{1}H NMR (300 MHz, $CDCl_3$, 25 °C, ppm): δ = 0.89 (t, ^3J = 6.6 Hz, 6 H, $H^{11d,11d'}$), 1.30 (m, 20 H, $H^{10c,10c'}$), 1.85 (m, 4 H, $H^{9b,9b'}$), 4.49 (t, ^3J = 6.6 Hz, 4 H, $H^{8a,8a'}$), 8.30 (d, ^3J = 4.7 Hz, 2 H, $H^{5,5'}$), 8.89 (s, 2 H, $H^{3,3'}$), 9.05 (d, ^3J = 4.7 Hz, 2 H, $H^{6,6'}$). FTIR (KBr, cm^{-1}): ν(C=O) 1732. $C_{28}H_{40}Cl_2N_2O_4Zn$ (604.92): calcd. C 55.40, H 6.66, N 4.63; found C 55.60, H 6.51, N 4.60.

(Dihexadecyl 2,2′-Bipyridyl-4,4′-dicarboxylate)zinc Chloride ([L²ZnCl₂], 8): Yield: 0.060 g, 72%. Thermotropic behaviour: Table 3. ^{1}H NMR (300 MHz, $CDCl_3$, 25 °C, ppm): δ = 0.88 (t, $^3J_{H,H}$ = 6.8 Hz, 6 H, $H^{11d,11d'}$), 1.26 (m, 52 H, $H^{10c,10c'}$), 1.85 (m, 4 H, $H^{9b,9b'}$), 4.49 (t, $^3J_{H,H}$ = 6.8 Hz, 4 H, $H^{8a,8a'}$), 8.30 (dd, $^3J_{H,H}$ = 5.1, $^4J_{H,H}$ = 1.2 Hz, 2 H, $H^{5,5'}$), 8.89 (s, 2 H, $H^{3,3'}$), 9.04 (d, $^3J_{H,H}$ = 5.1 Hz, 2 H, $H^{6,6'}$). FTIR (KBr, cm^{-1}): ν(C=O) 1733. $C_{44}H_{72}Cl_2N_2O_4Zn$ (829.35): calcd. C 63.72, H 8.75, N 3.38; found C 63.15, H 8.48, N 3.11.

(Didocosyl 2,2′-Bipyridyl-4,4′-dicarboxylate)zinc Chloride ([L³ZnCl₂], 9): Yield: 0.084 g, 72%. Thermotropic behaviour: Table 3. ^{1}H NMR (300 MHz, $CDCl_3$, 25 °C, ppm): δ = 0.88 (t, $^3J_{H,H}$ = 6.7 Hz, 6 H, $H^{11d,11d'}$), 1.25 (m, 76 H, $H^{10c,10c'}$), 1.85 (m, 4 H, $H^{9b,9b'}$), 4.49 (t, $^3J_{H,H}$ = 6.7 Hz, 4 H, $H^{8a,8a'}$), 8.30 (d, $^3J_{H,H}$ = 5.3 Hz, 2 H, $H^{5,5'}$), 8.89 (s, 2 H, $H^{3,3'}$), 9.04 (d, $^3J_{H,H}$ = 5.3 Hz, 2 H, $H^{6,6'}$). FTIR (KBr, cm^{-1}): ν(C=O) 1732. $C_{56}H_{96}Cl_2N_2O_4Zn$ (997.68): calcd. C 67.42, H 9.70, N 2.81; found C 67.32, H 9.41, N 2.79.

Synthesis of [L²MX₂] Complexes 10−15: The [L^2MX_2] complexes, starting from suitable precursors [L^2MCl_2] (M = Pd, Pt), were prepared by metathetical reactions with appropriate salts AX (X = I, Br, N_3). The synthesis of the [L^2PdI_2] (**10**) complex is described in detail; all other complexes were prepared in a similar fashion and only reagents, yields, solvents, ^{1}H NMR, IR, and analytical data are reported.

(Dihexadecyl 2,2′-Bipyridyl-4,4′-dicarboxylate)palladium(II) Iodide ([L²PdI₂], 10): KI (0.096 g, 0.58 mmol) was added to a yellow solution of [L^2PdCl_2], (**II**) (0.05 g, 0.058 mmol) in acetone (10 mL). The resultant suspension was then stirred at room temperature for 24 h. The so-obtained brown solid was filtered off and purified by recrystallization from chloroform/acetone to give the pure dark red product as a solid (0.050 g, 82%). Thermotropic behaviour: Table 4. ^{1}H NMR (300 MHz, $CDCl_3$, 25 °C, ppm): δ = 0.88 (m, 6 H, $H^{11d,11d'}$), 1.26 (m, 52 H, $H^{10c,10c'}$), 1.86 (m, 4 H, $H^{9b,9b'}$), 4.48 (t, $^3J_{H,H}$ = 6.8 Hz, 4 H, $H^{8a,8a'}$), 8.14 (d, $^3J_{H,H}$ = 5.9 Hz, 2 H, $H^{5,5'}$), 8.70 (s, 2 H, $H^{3,3'}$), 10.18 (d, $^3J_{H,H}$ = 5.9 Hz, 2 H, $H^{6,6'}$). FTIR (KBr, cm^{-1}): ν(C=O) 1729. $C_{44}H_{72}I_2N_2O_4Pd$ (1053.30): calcd. C 50.17, H 6.89, N 2.66; found C 50.50, H 7.51, N 3.25.

(Dihexadecyl 2,2′-Bipyridyl-4,4′-dicarboxylate)platinum(II) Iodide ([L²PtI₂], 11): 10 equiv. of KI; three days. Red product obtained from chloroform/methanol (0.082 g, 86%). Thermotropic behaviour: Table 4. ^{1}H NMR (300 MHz, $CDCl_3$, 25 °C, ppm): δ = 0.88 (t, $^3J_{H,H}$ = 6.9 Hz, 6 H, $H^{11d,11d'}$), 1.26 (m, 52 H, $H^{10c,10c'}$), 1.86 (m, 4 H, $H^{9b9b'}$), 4.48 (t, $^3J_{H,H}$ = 6.9 Hz, 4 H, $H^{8a,8a'}$), 8.12 (d, $^3J_{H,H}$ = 6.05 Hz, 2 H, $H^{5,5'}$), 8.63 (s, 2 H, $H^{3,3'}$), 10.51 (d, $^3J_{H,H}$ = 6.05 Hz, 2 H, $H^{6,6'}$). FTIR (KBr, cm^{-1}): ν(C=O) 1720. $C_{44}H_{72}I_2N_2O_4Pt$ (1141.96): calcd. C 46.28, H 6.36, N 2.45; found C 46.60, H 6.24, N 2.56.

(Dihexadecyl 2,2′-Bipyridyl-4,4′-dicarboxylate)palladium(II) Bromide ([L²PdBr₂], 12): 20 equiv. of KBr; DMF; three days. Yellow product obtained from chloroform/methanol (0.054 g, 80%). Thermotropic behaviour: Table 4. ^{1}H NMR (300 MHz, $CDCl_3$, 25 °C, ppm): δ = 0.88 (t, $^3J_{H,H}$ = 6.7 Hz, 6 H, $H^{11d,11d'}$), 1.26 (m, 52 H, $H^{10c,10c'}$), 1.85 (m, 4 H, $H^{9b,9b'}$), 4.48 (t, $^3J_{H,H}$ = 6.7 Hz, 4 H, $H^{8a,8a'}$), 8.11 (d, $^3J_{H,H}$ = 6.1 Hz, 2 H, $H^{5,5'}$), 8.66 (s, 2 H, $H^{3,3'}$), 9.85 (d, $^3J_{H,H}$ = 6.1 Hz, 2 H, $H^{6,6'}$). FTIR (KBr, cm^{-1}): ν(C=O) 1722. $C_{44}H_{72}Br_2N_2O_4Pd$ (959.29): calcd. C 55.09, H 7.57, N 2.92; found C 54.79, H 7.11, N 2.43.

(Dihexadecyl 2,2′-Bipyridyl-4,4′-dicarboxylate)platinum(II) Bromide ([L^{2}PtBr$_2$], 13): 20 equiv. of KBr; DMF; four days. Yellow product obtained from chloroform/methanol (0.066 g, 76%). Thermotropic behaviour: Table 4. ^{1}H NMR (300 MHz, $CDCl_3$, 25 °C, ppm): δ = 0.88 (t, $^3J_{H,H}$ = 6.6 Hz, 6 H, H$^{11d,11d'}$), 1.26 (m, 52 H, H$^{10c,10c'}$), 1.86 (m, 4 H, H$^{9b,9b'}$), 4.47 (t, $^3J_{H,H}$ = 6.6 Hz, 4 H, H$^{8a,8a'}$), 8.11 (d, $^3J_{H,H}$ = 5.8 Hz, 2 H, H$^{5,5'}$), 8.60 (s, 2 H, H$^{3,3'}$), 10.23 (d, $^3J_{H,H}$ = 5.8 Hz, 2 H, H$^{6,6'}$). FTIR (KBr, cm^{-1}): ν(C=O) 1730. $C_{44}H_{72}Br_2N_2O_4Pt$ (1047.95): calcd. C 50.43, H 6.93, N 2.67; found C 50.14, H 6.75, N 2.32.

(Dihexadecyl 2,2′-Bipyridyl-4,4′-dicarboxylate)palladium(II) Azide ([L^{2}Pd(N$_3$)$_2$], 14): 10 equiv. of NaN_3; 24 h. Yellow product obtained from chloroform/acetone (0.033 g, 65%). Thermotropic behaviour: Table 4. ^{1}H NMR (300 MHz, $CDCl_3$, 25 °C, ppm): δ = 0.88 (t, $^3J_{H,H}$ = 6.5 Hz, 6 H, H$^{11d,11d'}$), 1.26 (m, 52 H, H$^{10c,10c'}$), 1.86 (m, 4 H, H$^{9b,9b'}$), 4.47 (t, $^3J_{H,H}$ = 6.5 Hz, 4 H, H$^{8a,8a'}$), 8.145 (d, $^3J_{H,H}$ = 5.5 Hz, 2 H, H$^{5,5'}$), 8.67 (s, 2 H, H$^{3,3'}$), 8.81 (d, $^3J_{H,H}$ = 5.5 Hz, 2 H, H$^{6,6'}$). FTIR (KBr, cm^{-1}): ν(C=O) 1728, ν(N_3) 2043. $C_{44}H_{72}N_8O_4Pd$ (883.53): calcd. C 59.82, H 8.21, N 12.68; found C 60.01, H 8.69, N 12.32.

(Dihexadecyl 2,2′-Bipyridyl-4,4′-dicarboxylate)platinum(II) Azide ([L^{2}Pt(N$_3$)$_2$], 15): 10 equiv. of NaN_3; 48 h. Orange product obtained from chloroform/methanol (0.036 g, 45%). Thermotropic behaviour: Table 4. ^{1}H NMR (300 MHz, $CDCl_3$, 25 °C, ppm): δ = 0.88 (t, $^3J_{H,H}$ = 6.6 Hz, 6 H, H$^{11d,11d'}$), 1.26 (m, 52 H, H$^{10c,10c'}$), 1.86 (m, 4 H, H$^{9b,9b'}$), 4.47 (t, $^3J_{H,H}$ = 6.6 Hz, 4 H, H$^{8a,8a'}$), 8.10 (d, $^3J_{H,H}$ = 5.9 Hz, 2 H, H$^{5,5'}$), 8.63 (s, 2 H, H$^{3,3'}$), 9.14 (d, $^3J_{H,H}$ = 5.9 Hz, 2 H, H$^{6,6'}$). FTIR (KBr, cm^{-1}): ν(C=O) 1728, ν(N_3) 2063. $C_{44}H_{72}N_8O_4Pt$ (972.19): calcd. C 54.36, H 7.46, N 11.53; found C 54.04, H 7.20, N 11.40.

CCDC-208739 and CCDC-208740 contain the supplementary crystallographic data for this paper. These data can be obtained free of charge at www.ccdc.cam.ac.uk/conts/retrieving.html [or from the Cambridge Crystallographic Data Centre, 12 Union Road, Cambridge CB2 1EZ, UK; Fax: (internat.) +44−1223/336-033; E-mail: deposit@ccdc.cam.ac.uk].

Acknowledgments

This work was partly supported by CIPE grants (Clusters 14 and 26) from the Ministero dell'Istruzione, dell'Università e della Ricerca.

[1] J. L. Serrano, *Metallomesogens*, VCH, Weinheim, **1996**.
[2] B. Donnio, D. W. Bruce, *Structure and Bonding*, (Ed.: D. M. P. Mingos, Vol. 95, Liquid Crystals II. Metallomesogens, Springer, **1999**.
[3] H. Richtzenhain, A. J. Blake, D. W. Bruce, I. A. Fallis, W. Li, M. Schroder, *Chem. Commun.* **2001**, 2580−2581.
[4] I. Aiello, M. Ghedini, M. La Deda, D. Pucci, O. Francescangeli, *Eur. J. Inorg. Chem.* **1999**, 1367−1372.
[5] T. Hegmann, F. Peidis, S. Diele, C. Tschierske, *Liq. Cryst.* **2000**, *27*, 1261−1265.
[6] M. Benouazzane, S. Coco, P. Espinet, J. Barbera, *J. Mater. Chem.* **2001**, *11*, 1740−1744.
[7] S. T. Trzaska, T. M. Swager, *Chem. Mater.* **1998**, *10*, 438−443.
[8] S. Coco, F. Diez-Exposito, P. Espinet, C. Fernandez-Mayordomo, J. M. Martin-Alvarez, A. M. Levelut, *Chem. Mater.* **1998**, *10*, 3666−3671.
[9] C. Yang, Y. Pang, C. K. Lai, *Liq. Cryst.* **2001**, *28*, 191−195.
[10] K. E. Rowe, D. W. Bruce, *Liq. Cryst.* **1996**, *20*, 183−193.
[11] C. Tschierske, *Angew. Chem. Int. Ed.* **2000**, *39*, 2454−2458.
[12] O. Maury, J.-P. Guégan, T. Renouard, A. Hilton, P. Dupau, N. Sandon, L. Toupet, H. Le Bozec, *New J. Chem.* **2001**, *25*, 1553−1566.
[13] R. Ziessel, *Coord. Chem. Rev.* **2001**, *216−217*, 195−223 and references therein.
[14] S. S. Kamath, V. Uma, T. S. Srivastava, *Inorg. Chim. Acta* **1989**, *161*, 49−56.
[15] D. Pucci, G. Barberio, A. Crispini, O. Francescangeli, M. Ghedini, *Mol. Cryst. Liq. Cryst.* **2003**, *395*, 325−335.
[16] T. J. Nelson, J. R. Wullert II, *Electronic Information Display Technologies*, World Scientific Publishing,Singapore, **1997**.
[17] [17a] H. J. Coles, *Liq. Cryst.* **1993**, *14*, 1039−1042. [17b] R. Yamaguchi, J. Kishida, S. Sato, *Jpn. J. Appl. Phys.* **2000**, *39*, 5235−5237.
[18] D. Song, Q. Wu, A. Hook, I. Kozin, S. Wang, *Organometallics* **2001**, *20*, 4683−4689.
[19] W. Lu, N. Zhu, C. Che, *Chem. Commun.* **2002**, 900−901.
[20] F. Neve, A. Crispini, C. Di Pietro, S. Campagna, *Organometallics* **2002**, *21*, 3511−3518 and references therein.
[21] [21a] G. R. Newkome, F. R. Fronczek, V. K. Gupta, W. E. Puckett, D. C. Pantaleo, G. E. Kiefer, *J. Am. Chem. Soc.* **1982**, *104*, 1782−1783. [21b] P. D. Beer, N. C. Fletcher, M. G. B. Drew, T. J. Wear, *Polyhedron* **1997**, *16*, 815−823.
[22] M. Maekawa, M. Munakata, S. Kitagawa, M. Nakamura, *Anal. Sci.* **1991**, *7*, 521−523.
[23] M. A. Khan, D. G. Tuck, *Acta Crystallogr., Sect. C* **1984**, *40*, 60−62.
[24] C. W. Reimann, S. Block, A. Perloff, *Inorg. Chem.* **1966**, *5*, 1185−1189.
[25] H.-L. Kwong, K.-M. Lau, W.-S. Lee, W.-T. Wong, *New. J. Chem.* **1999**, *23*, 629−632.
[26] K. Nakamoto, *Infrared and Raman Spectra of Inorganic and Coordination Compounds*, Wiley-Interscience, New York, 4th edn., pp. 231, 290−291, **1986**.
[27] J. Kaiser, J. Sieler, U. Braun, L. Golic, E. Dinjus, D. Walther, *J. Organomet. Chem.* **1982**, *224*, 81−87.
[28] D. W. Evans, G. R. Newkome, F. R. Fronczek, *Acta Crystallogr., Sect. C* **1990**, *46*, 490−491.
[29] T. J. Kinnunen, M. Haukka, T. T. Pakkanen, T. A. Pakkanen, *J. Organomet. Chem.* **2000**, *613*, 257−262.
[30] J. Goodby, in: *Phase Structures of Calamitic Liquid Crystals*, Vol. 2A. *Handbook of Liquid Crystals* (Eds.: D. Demus, J. Goodby, G. W. Gray, H.-W. Spiess, V. Vill); Weinheim: Wiley-VCH, **1998**.
[31] A. El-ghayoury, L. Douce, A. Skoulios, R. Ziessel, *Angew. Chem. Int. Ed.* **1998**, *37*, 1255−1258.
[32] D. Felder, B. Heinrich, D. Guillon, J.-F. Nicoude, J.-F. Nierengarten, *Chem. Eur. J.* **2000**, *6*, 3501−3507.
[33] S. Méry, D. Haristoy, J.-F. Nicoude, D. Guillon, S. Diele, H. Monobe, Y. Shimizu, *J. Mater. Chem.* **2002**, *12*, 37−41.
[34] E. J. L. McInnes, R. D. Farley, C. C. Rowlands, A. J. Welch, L. Rovatto, L. J. Yellowless, *J. Chem. Soc., Dalton Trans.* **1999**, 4203−4208.
[35] P. M. Gidney, R. D. Gillard, B. T. Haeton, *J. Chem. Soc., Dalton Trans.* **1973**, 132−134 and references therein.
[36] V. M. Houlding, V. M. Miskowski, *Coord. Chem. Rev.* **1991**, *111*, 145−152 and references therein.
[37] W. B. Connick, V. M. Miskowski, V. M. Houlding, H. B. Gray, *Inorg. Chem.* **2000**, *39*, 2585−2592 and references therein.
[38] V. M. Miskowski, V. H. Houlding, *Inorg. Chem.* **1989**, *28*, 1529−1533.
[39] V. Balzani, V. Carassiti, *Photochemistry of Coordination Compounds*, Academic Press, London, **1970**.
[40] [40a] M. Maestri, C. Deuschel-Cornioley, A. von Zelewsky, *Coord. Chem. Rev.* **1991**, *111*, 117−123. [40b] M. Maestri, V. Balzani, C. Deuschel-Cornioley, A. von Zelewsky, *Adv. Photochem.* **1992**, *17*, 1−68.
[41] [41a] V. M. Textor, H. R. Oswald, *Z. Anorg. Allg. Chem.* **1974**, *407*, 244−256. [41b] R. S. Osborn, D. Rogers, *J. Chem. Soc., Dalton Trans.* **1974**, 1002−10004.

[42] V. M. Miskowski, V. H. Houlding, C-M. Che, Y. Wang, *Inorg. Chem.* **1993**, *32*, 2518−2524.
[43] W. B. Connick, L. M. Henling, R. E. Marsh, H. B. Gray, *Inorg. Chem.* **1996**, *35*, 6261−6265.
[44] J. N. Demas, G. A. Crosby, *J. Phys. Chem.* **1971**, *93*, 2841−2844.
[45] K. Nakamaru, *Bull. Soc. Chem. Jpn.* **1982**, *5*, 2697−2705.
[46] A. C. T. North, D. C. Phillips, F. S. Mathews, *Acta Crystallogr., Sect. A* **1968**, *24*, 351−359.
[47] S. Parkin, B. Moezzi, H. J. Hope, *Appl. Crystallogr.* **1995**, *28*, 53−56.
[48] *SHELXTL*/*NT* crystal structure analysis package, Bruker AXS, Inc.: Madison, WI, **1999**.

Received April 17, 2003

